DE GRUYTER OPEN

Acta Geophysica
vol. 63, no. 2, Apr. 2015, pp. 451-467
DOI: 10.1515/acgeo-2015-0004

Influences of Al, Mg, and K on Calculating Concentrations of Other Formation Elements and Their Corrections in Geochemical Logging

Wensheng WU[1], Maosong TONG[2], Wei NIU[1], and Li LUO[3]

[1]State Key Laboratory of Petroleum Resource and Prospecting, China University of Petroleum, Beijing, China; e-mail: wwsheng@cup.edu.cn

[2]Daqing Drilling Corporation, PetroChina, Daqing, China

[3]CCDC Well Logging Company, Chongqing, China

A b s t r a c t

In geochemical logging, the standard capture gamma-ray spectra of Al, Mg, and K have no distinct characteristic energy peaks. This feature easily influences the spectral bands of characteristic peaks of other elements and thus affects the accuracy of calculating their concentrations. To study this influence, we constructed a model formation containing Al, Mg, and K, and employed the Monte Carlo N Particle Transport Code (MCNP) program to simulate their capture spectra. The results indicate that the calculated dry weights of Si are almost free from the influences of Mg, K, and Al. The ones of Ca and Fe are influenced, but only to a minor extent. The dry weight of S is concurrently influenced. Specifically, the K concentration causes S concentration to deviate significantly from its real concentration. By correcting for such influences, we can obtain relatively accurate values. Data processing for a real well validates the finding that Mg, Al, and K in the formation influence the precision of calculation of other elements and also testifies to the effectiveness of the correction method.

Key words: geochemical elemental logging, spectral stripping, elemental concentration.

1. INTRODUCTION

In geochemical logging, fast neutrons emitted from neutron source enter the formation to collide with nuclides in the formation, leading to three kinds of prompt nuclear reactions, *i.e.*, inelastic scattering, capture, and particle reactions. In all three cases, the resultant nucleus in an excited state decays and yields gamma rays with energies which are characteristic of the particular nucleus in the formation. Therefore, we can discriminate types of formation elements by detecting gamma-ray energy and determine the elemental content by measuring the intensity of specific-energy gamma rays. Because the measurement spectrum of a formation can be assumed as a linear superposition of the standard spectra of all elements in the formation in certain portions which add up to 1, with the standard elemental gamma-ray spectra, we can directly quantitatively analyze the mixed gamma-ray spectra of the measured formation to obtain the element's relative yields which are not the actual elemental weight percent or dry weight in the formation and cannot be directly used to evaluate the formation's mineralogy. The conversion factor between elemental relative yield and its dry weight is just the detection sensitivity factor (or sensitivity factor in short). Then, according to the sensitivity factor of each element in the formation and the formation oxide closure model, the weight percent or dry weight of every major element in the rock matrix is obtained, so as to further identify mineral composition of the rock matrix. In actual logging, the internal media in a well will influence the measured formation spectrum. When the internal fluid in a well has a high mineral salt concentration, the available formation signal in the measured spectrum degrades, since the elemental Cl in the fluid is a major neutron absorber, whereas the statistical uncertainty increases. Barite in the internal fluid in a well is a gamma-ray absorber and will deform the measured spectrum. So, the calculated relative yields need to be corrected for these influences before they are used to calculate elemental dry weights (Ellis and Singer 2008, Helmer *et al.* 1967, Hertzog *et al.* 1989, Herron 1986, Chapman *et al.* 1987, Grau and Schweitzer 1989, Galford *et al.* 2009).

When the source is Am-Be-source, geochemical logging usually utilizes the capture gamma-ray spectra to gain the elemental relative yields and dry weights. The main elements measured with this source include silicon, calcium, iron, sulfur, titanium, gadolinium, aluminum, magnesium, and potassium, among which silicon, calcium, iron, sulfur, titanium, and gadolinium are the six important elements indicative of formation minerals, having large capture cross-sections and distinct characteristic peaks in standard spectra, so their concentrations can be directly obtained from analysis of the capture gamma-ray spectra. Hydrogen and chlorine neutron capture signals are also detected, but they are not used for mineralogical evaluations.

One important reason for calculating concentrations of different elements through quantitative analysis of energy spectra is the differences in standard spectra of different elements. The more unique a feature an element's standard capture gamma-ray spectrum has, the better the measurability of the element. For elements with similar standard gamma-ray spectra, it is very difficult to calculate their concentrations through energy spectral analysis precisely. The three skeleton elements, *i.e.*, aluminum, magnesium, and potassium, have no distinct characteristic peaks in their standard spectra, making it difficult to obtain their concentrations from analysis of mixed formation spectra against their standard spectra; the standard capture gamma-ray spectra of these three elements are shown in Fig. 1. As can be seen from Fig. 1, neither Mg nor K has a very distinct characteristic peak. Al has no distinct characteristic peak other than a characteristic peak at 7.70 MeV, which is very close to 7.64 and 7.28 MeV, the strong energy peaks of Fe. Therefore, during Am-Be-source chemical elemental logging, the concentrations of elements Mg, Al, and K in the formation cannot be obtained through an analysis of capture spectra; instead, they have to be obtained by using other gamma-ray energy spectra logging methods. The new tool solutions, which are committed to improve the signal-to-noise ratio of formation responses by reducing undesired borehole and tool contributions, increase the energy resolution of spectra important for better differentiation of elements, which solves the identification of Al, Mg, and K to some extent (Galford *et al.* 2009, Radtke *et al.* 2012).

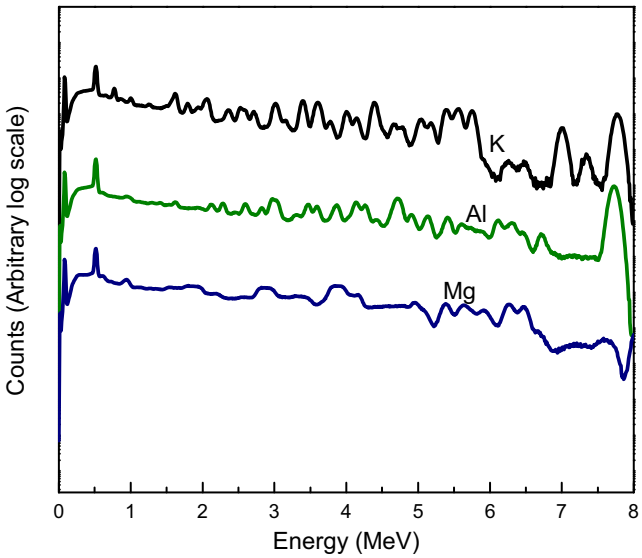

Fig. 1. Capture spectra of elements Mg, Al, and K.

MCNP5C, which can track photons according to the originating isotope, was used to carry out calculations for zero- and medium-porosity sandstone, limestone, and dolomite formations. On the basis of the detector response function, the MCNP5 simulation formation spectral responses for a geochemical tool can produce the best match to laboratory measurements made in quarried and fabricated rock formations. So, in this paper we employ the MCNP5 program (Sweezy *et al*. 2004) to study the influences of Al, Mg, and K on the results of analysis of the four important elements, Si, Ca, S, and Fe, in some model formation for GEM tool (Galford *et al.* 2009) that introduces additional hardware innovations to improve the signal-to-noise ratio of formation responses by reducing undesired borehole and tool contributions. The simulation results are used for developing corresponding correction methods. The processing of real well data will validate the effectiveness of the corrections.

2. FORMATION NOT CONTAINING MG, AL, AND K

The simulation model is a cylinder with a height of 2000 mm and a diameter of 1600 mm. The borehole well diameter is 200 mm, and the in-hole fluid is fresh water. The GEM tool that consists of A standard chemical americium-beryllium neutron source and a large bismuth germanate (BGO) detector located above the source is put against the well wall. Since the tally mode F8 in MCNP5 is the tally of electronic pulse energy amplitude that records gamma ray energy deposition in formation tally cell, the count by F8 is more suitable for spectral logging, and close to the count of the actual logging instrument compared to other tally modes. Here F8 is used to record the induced capture gamma-ray spectra of BGO detector.

The formation swas deemed to be one entity filled with different volumes of SiO_2, $CaCO_3$, $FeCO_3$, $CaSO_4$, and H_2O; the major skeleton elements in the formation are Si, Ca, Fe, and S, as shown in Table 1.

Table 1

Volume contents of minerals in strata containing Si, Ca, Fe, and S

Model	Density [g/cm^3]	Mineral volume content [%]				
		SiO_2	$CaCO_3$	$CaSO_4$	$FeCO_3$	H_2O
1	2.589	50	25	10	5	10
2	2.690	45	30	15	5	5
3	2.639	60	15	10	7	8
4	2.597	65	20	5	3	7
5	2.577	30	50	3	6	11
6	2.548	20	45	20	2	13
7	2.545	27	26	12	15	20

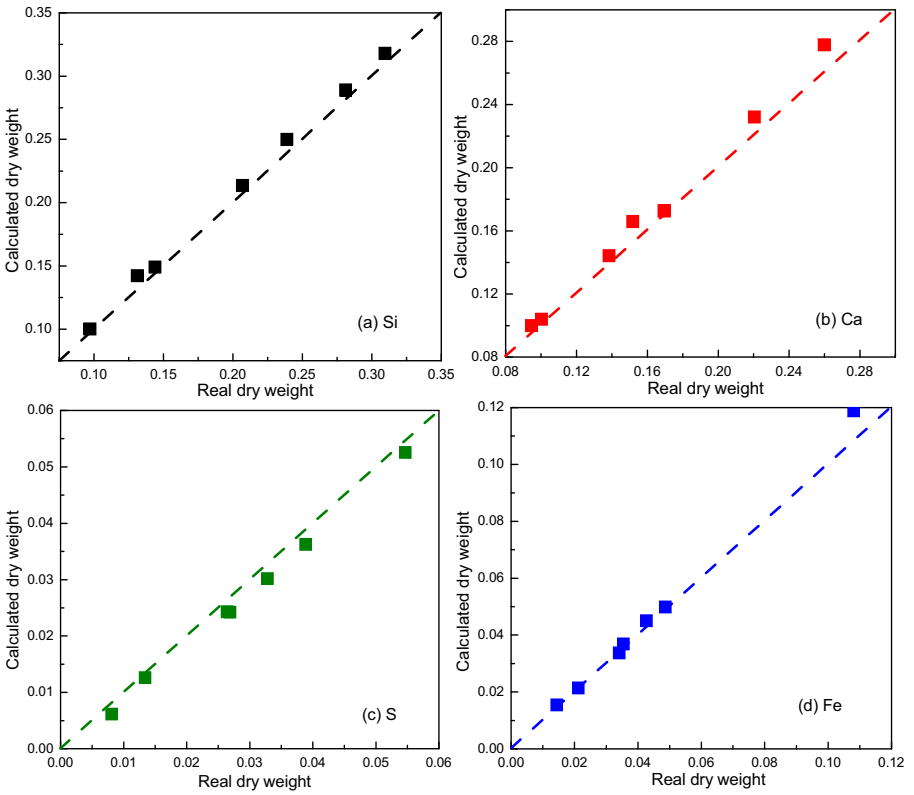

Fig. 2. Comparison between real dry weight and calculated dry weight of formation elements in Table 1.

A constrained and weighted least-squares method is used to analyze simulated capture gamma-ray spectra of seven formations listed in Table 1 to get elemental relative yields because the method can ensure that physically feasible solutions are obtained for the individual contributions, or elemental yields. We obtained the relative yields of four elements, Si, Ca, Fe, and S; then, according to the detection sensitivity factors of these four elements and depth normalization factors of the seven formations (Ellis and Singer 2008, Pang 1991, Pemper *et al.* 2006, Herron *et al.* 2002), we calculated the dry weights of Si, Ca, Fe, and S. Dry weights of four elements obtained from spectral analysis were compared with real dry weights of various elements in the formation, as shown in Fig. 2, in which the diagonal dashed lines are the equivalent lines of calculated values and real values of the formation. As can be seen in Fig. 2, the dry weights of Si, Ca, Fe, and S obtained from the spectral analysis have generally high precision, and their correlation coefficients relative to real values reach more than 0.998. Such high-precision

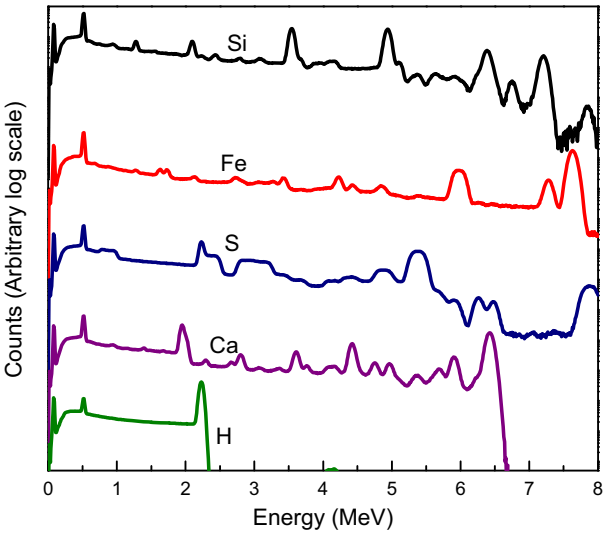

Fig. 3. Capture spectra of elements H, Si, Ca, Fe, and S.

spectral analysis results are attributed to the quantitative analysis method and to the important fact that, in standard spectra of the major elements H, Si, Ca, Fe, and S, there is little interference among characteristic peaks. For example, Ca's full-energy peaks at 1.94 and 4.42 MeV, Si's full-energy peak at 3.54 MeV, S's full-energy peak at 5.40 MeV, and Fe's full-energy peaks at 5.92 and 7.64 MeV are very distinct, with independent peak positions and high intensities, as shown in Fig. 3.

3. SPECTRAL ANALYSIS RESULTS OF THE FORMATION CONTAINING MG, AL, AND K

Mg-bearing formation

The formation volume was deemed to be 1, with different volumes of SiO_2, $CaCO_3$, $FeCO_3$, $CaSO_4$, and H_2O. A certain volume of dolomite ($CaMg(CO_3)_2$) was added to the formation. The mineral volume contents of the formation models are shown in Table 2. Skeleton elements in these formation models include H, Si, Ca, S, Fe, and Mg.

According to the standard spectrum and detection sensitivity factor of each element and depth normalization factor of each formation, the mixed neutron-capture gamma-ray spectra of these formations were analyzed to get the dry weight of each element. Because Mg has no distinct characteristic peak, its concentration cannot be obtained from analysis of neutron-capture gamma-ray energy spectra. The dry weight of Mg has to be determined from

Table 2

Volume contents of minerals in complicated Mg-bearing strata

Model	Density [g/cm^3]	Mineral volume content [%]					
		SiO_2	$CaCO_3$	$CaMg(CO_3)_2$	$CaSO_4$	$FeCO_3$	H_2O
1	2.571	70	6	6	6	3	9
2	2.625	65	8	14	5	2	6
3	2.654	60	10	9	8	6	7
4	2.663	55	12	17	9	2	5
5	2.555	50	15	12	7	4	12
6	2.590	45	18	16	8	3	10
7	2.652	40	20	25	5	3	7
8	2.716	35	28	23	6	4	4
9	2.732	30	39	4	11	10	6
10	2.677	25	18	35	4	8	10
11	2.596	20	40	10	3	12	15
12	2.784	15	30	30	15	6	4
13	2.668	10	11	60	7	2	10
14	2.629	5	60	13	7	5	10

the lithology index P_e for litho-density logging. Assuming that the dry weight of Mg in the formation has been obtained, we can calculate the dry weights of elements Si, Ca, Fe, and S in various formations listed in Table 2 by using an analytical algorithm. The results are shown in Fig. 4.

As can be seen from Fig. 4, the three elements, Si, Ca, and Fe, in the Mg-bearing formation still have very high spectral analysis precision, with correlation coefficients between the calculated and real dry weights reaching about 0.99, but S has a distinctly lower spectral analysis precision, with the calculated value points distinctly deviated from the diagonal line. The analysis of the standard spectra of elements Si, Ca, and Fe shows that each standard spectrum has two or more strong characteristic energy peaks that can be easily identified. Mg has little influence on the characteristic peak counts of these three elements; thus, Si, Ca, and Fe still have relatively high spectral analysis precision, being almost immune to the influence of Mg. Nevertheless, it can be known from the standard spectra of S that the strongest characteristic peak is only one peak at 5.4 MeV, whereas the other characteristic peaks are relatively gentle or overlap with peaks of other elements, and the strongest characteristic peak of S at 5.4 MeV is of very weak contrast to those of Si, Ca, and Fe. Thus, the influence of the complicated and variable energy spectrum of Mg on the counts of the S characteristic peak will rela-

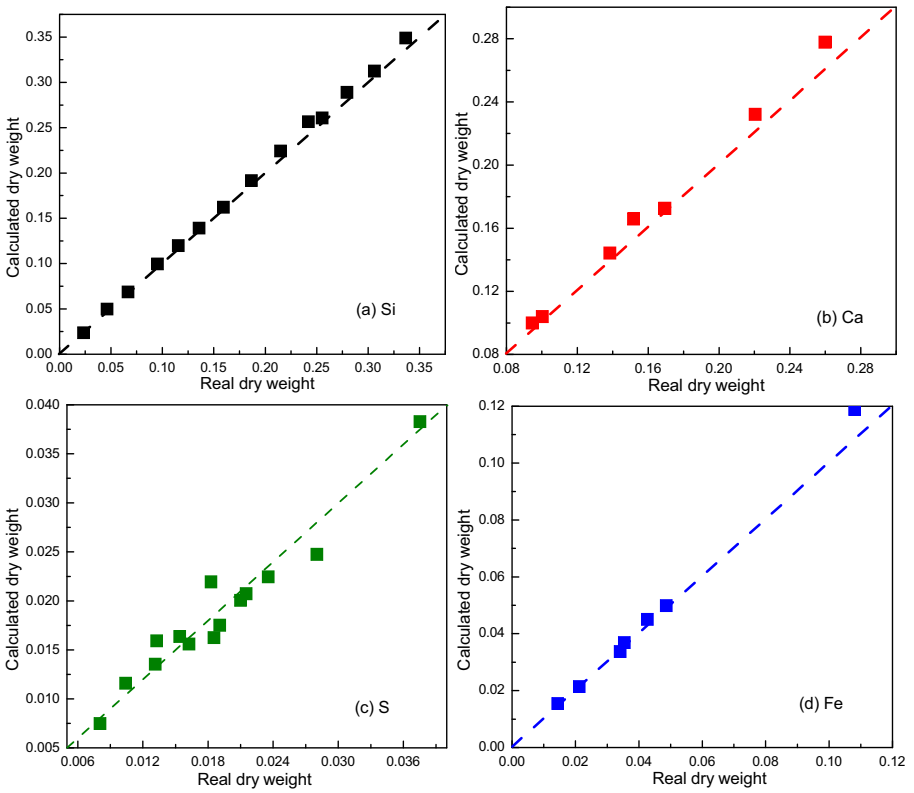

Fig. 4. Relationship of elemental concentration calculated from analysis of Mg-bearing formation *versus* real concentration.

tively increase, lowering the spectral analysis precision of S. However, since Mg appears relatively weak at 5.40 MeV, its influence on calculating S concentration is not great.

Formation containing Mg and Al

Deemed as one entity, the formation contains different volumes of SiO_2, $CaCO_3$, $FeCO_3$, $CaSO_4$, $CaMg(CO_3)_2$, and H_2O, plus a certain volume of anorthite ($CaAl_2Si_2O_8$). The mineral volume contents in the formation models are shown in Table 3. These formation models are based on those in Table 2, with Al added to their skeletons.

Assuming that concentrations of elements Mg and Al have been obtained, respectively, from the index P_e for litho-density logging and neutron aluminum activation logging (Herron and Herron 1996), we analyzed the mixed neutron-capture gamma-ray spectra of the above formation according

Table 3

Volume contents of minerals in Al-bearing strata

Model	Density [g/cm^3]	Mineral volume content [%]						
		SiO_2	$CaCO_3$	$CaMg(CO_3)_2$	$CaAl_2Si_2O_8$	$CaSO_4$	$FeCO_3$	H_2O
1	2.574	64	6	6	6	6	3	9
2	2.628	57	8	14	8	5	2	6
3	2.659	48	10	9	12	8	6	7
4	2.669	39	12	17	16	9	2	5
5	2.619	30	15	15	20	7	4	9
6	2.600	22	18	16	23	8	3	10
7	2.662	14	20	25	26	5	3	7
8	2.704	22	21	14	29	6	4	4
9	2.685	26	15	4	32	11	6	6
10	2.653	11	13	19	35	4	8	10
11	2.626	12	25	10	38	3	4	8
12	2.755	9	10	15	41	15	6	4
13	2.618	2	4	31	44	7	2	10
14	2.688	3	31	3	47	6	5	5

to the standard spectrum and detection sensitivity factor of each element and depth normalization factor of each formation, and we obtained the dry weight of each element, as shown in Fig. 5.

As can be seen from Fig. 5, Si concentration still has a relatively high spectral analysis precision. Compared with Fig. 4, at a high concentration of Ca, the calculated values deviate farther from the diagonal line and thus the spectral analysis precision decreases; for Fe, the calculated values deviate farther from the diagonal line, too, indicating that the spectral analysis precision of Fe concentration decreases. This can be explained from Fig. 6, which shows neutron-capture gamma-ray energy spectra of the SiO_2–$CaCO_3$ mixed formation and the SiO_2–$CaAl_2Si_2O_8$ mixed formation, where the Al-bearing stratum enables lower characteristic peaks of Ca, which causes the reduced spectral analysis precision of Ca concentration. The characteristic peak of Al at 7.70 MeV influences one characteristic peak of Fe, which is the cause of the reduced spectral analysis precision of Fe concentration. The lower the Fe concentration in the formation, the greater the influence of Al on the calculated Fe concentration. Compared with complicated Mg-bearing formation, the spectral analysis precision of S in the complicated formation containing Mg and Al does not vary much; as a whole, the calculated dry weight of S is kept consistent with its real dry weight. This indicates that, despite Mg and

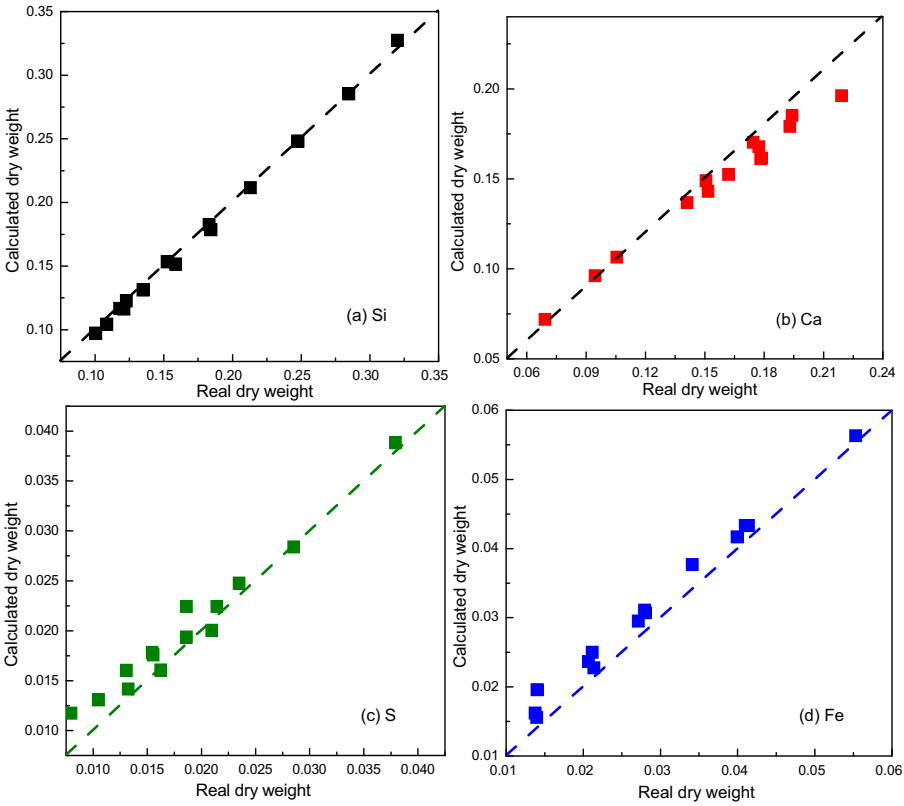

Fig. 5. Comparison between real dry weight and calculated dry weight of each element in Al-bearing formation.

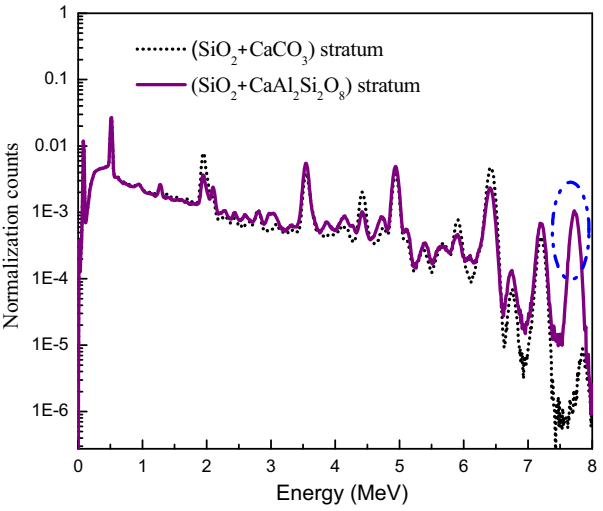

Fig. 6. Mixed capture energy spectra of the Al-bearing and non-Al-bearing formation.

Al inducing an interfering peak effect on S and lowering the spectral analysis precision of S such an influence is not especially great.

Formation containing Mg, Al, and K

Deemed as one entity, the formation contains different volumes of SiO_2, $CaCO_3$, $FeCO_3$, $CaSO_4$, $CaMg(CO_3)_2$, and H_2O, plus a certain volume of orthoclase ($KAlSi_3O_8$). The mineral volume contents of the various formation models are shown in Table 4. Besides H, Si, Ca, Fe, and S, the formation contains three more elements: Mg, Al, and K.

Table 4

Volume contents of minerals in complicated K-bearing strata

Model	Density [g/cm^3]	Mineral volume content [%]						
		SiO_2	$CaCO_3$	$CaMg(CO_3)_2$	$KAlSi_3O_8$	$CaSO_4$	$FeCO_3$	H_2O
1	2.566	64	6	6	6	6	3	9
2	2.618	57	8	14	8	5	2	6
3	2.643	48	10	9	12	8	6	7
4	2.649	39	12	17	16	9	2	5
5	2.593	30	15	15	20	7	4	9
6	2.570	22	18	16	23	8	3	10
7	2.628	14	20	25	26	5	3	7
8	2.666	22	21	14	29	6	4	4
9	2.643	26	15	4	32	11	6	6
10	2.608	11	13	19	35	4	8	10
11	2.576	12	25	10	38	3	4	8
12	2.702	9	10	15	41	15	6	4
13	2.561	2	4	31	44	7	2	10
14	2.627	3	31	3	47	6	5	5

After the concentrations of K, Mg, and Al are gained, respectively, from natural gamma-ray spectral logging, the P_e logging and aluminum activation logging (Herron and Herron 1996), the neutron-capture gamma-ray energy spectra data of these formations were analyzed, and the obtained relative yields of elements were converted to dry weight of each respective element, as shown in Fig. 7.

Compared with Fig. 5, elements Si, Ca, and Fe in Fig. 7 have higher spectral analysis precision, with smaller differences between calculated dry weight and real one. This is because the energy spectra of Si, Ca, and Fe have many intense characteristic peaks, and any of these three elements in

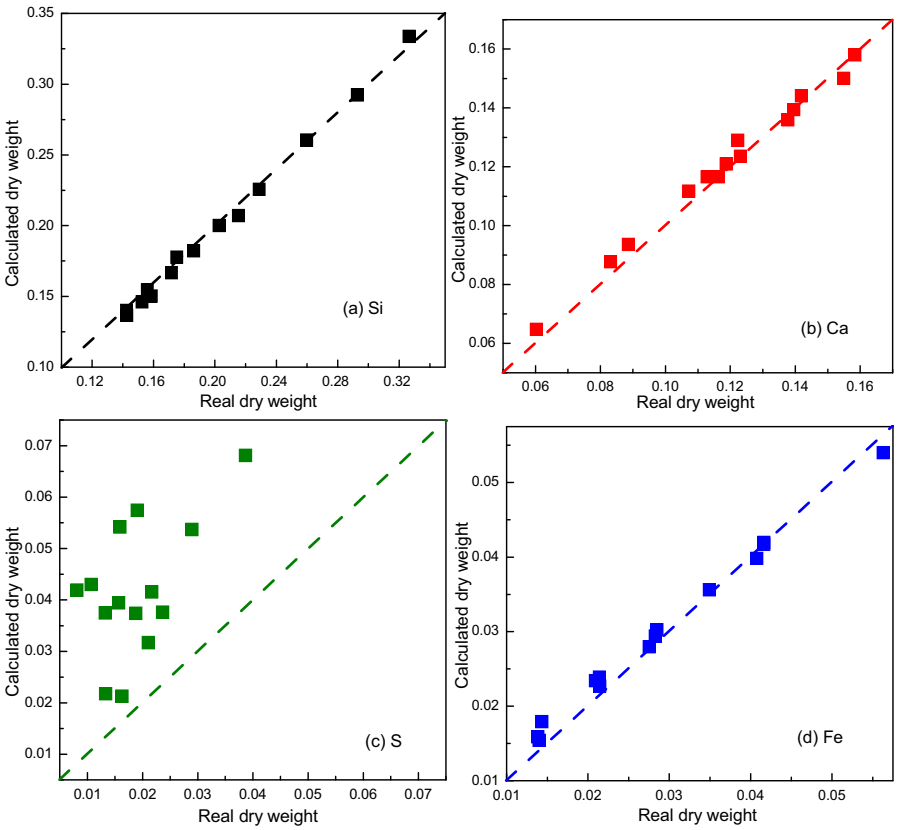

Fig. 7. Comparison between theoretical and real values of each element in complicated K-bearing formation.

formation can generally keep at least one independent characteristic peak immune to interference from other elements and less affected by K. Al has one characteristic peak overlapping with one of Fe's characteristic peaks, but it does not exert much influence on the spectral analysis result of Fe. Figure 7 clearly shows a greatly reduced spectral analysis precision of S, with the correlation coefficient between calculated dry weight and real dry weight falling to below 0.6, and calculated values of S are distinctly greater than the real values, which are considered to be distorted. This can be explained from Fig. 8, showing capture gamma-ray energy spectra of two formations: one composed of SiO_2 and $CaCO_3$, and the other composed of SiO_2, $CaCO_3$, and $KAlSi_3O_8$. The characteristic spectral band 5.0-6.0 MeV of K in the K-bearing energy spectra induces intense interference upon S's characteristic peak at 5.40 MeV and increases the characteristic peak count of S. In fact, some of the counts of this enhanced characteristic peak of S originate from

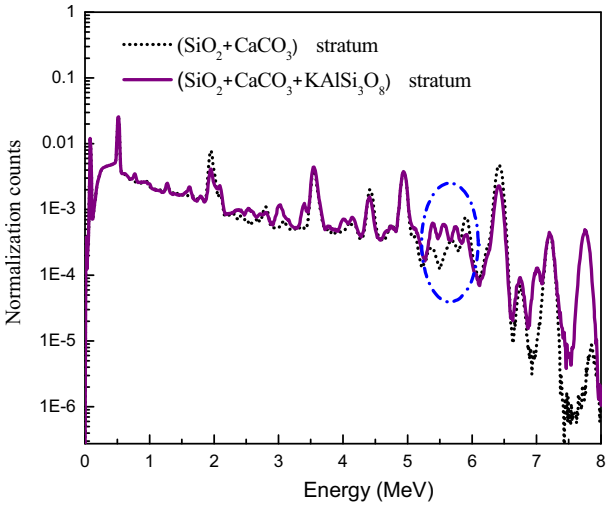

Fig. 8. Mixed capture energy spectra of K-bearing and non-K-bearing formations.

the characteristic peak count of K. For S, except for a distinct characteristic peak at 5.40 MeV, no other strong characteristic peak can control its spectra; thus, the spectral analysis result is greatly distorted.

4. INFLUENCE CORRECTIONS

Taking Fig. 7c as an example where K distorts the spectral analysis accuracy of S, we subtracted the real dry weight of S in the formation from the calculated dry weight derived from spectral analysis to get the difference *D*, and with the difference *D* as the ordinate and the real dry weight of K in the formation as the abscissa, we obtained the result shown in Fig. 9. As can be seen from Fig. 9, with increasing K concentration, the difference between the calculated dry weight and the real dry weight of S exhibits a linear increase, indicating that this part of the difference is primarily caused by the influence of K concentration in the formation.

A fitting of data points in Fig. 9 gives rise to a linear expression for the difference between calculated dry weight and real dry weight of S *versus* K concentration in the formation. With this relationship expression, we can correct the calculated dry weight of S according to the real dry weight of K in the formation. Correction of the calculated dry weight of S in Fig. 7c gives rise to the relationship between corrected S concentration and real dry weight, as shown in Fig. 10. Therefore, the corrected dry weight of S is relatively close to the real dry weight of S in the formation, indicating that this correction method is relatively effective. There is still a certain deviation be-

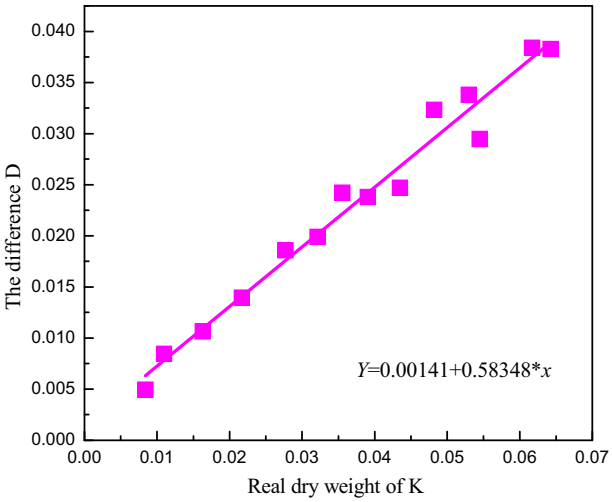

Fig. 9. Influence of K concentration on calculated value of S.

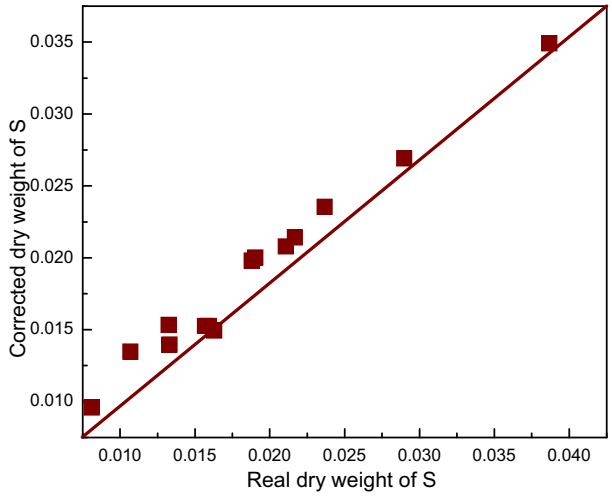

Fig. 10. Comparison between corrected dry weight and real dry weight of S.

tween the corrected dry weight and the real dry weight of S, because the influences of Al and Mg on S are still present. If influences of Al and Mg are further corrected for according to the above method, then the corrected dry weight will further approach its real dry weight. It should be noted that the concentration of Al, Mg, or K influences the concentration calculation of elements Ti and Gd besides those of Si, Ca, S, and Fe, which needs to be investigated.

It need be emphasized that the correction method is dependent not only on the level of disturbing elements, but also on the level of the main tested elements. As a consequence, the method can give the true correction in a limited range of tested elements.

5. FIELD EXAMPLE

Chlorine in the borehole or formation fluid degrades the usable formation signals in the measured spectra and increases the statistical uncertainty for its major neutron absorber. Barite in the internal fluid in a well, a gamma-ray absorber, will deform the measured spectrum. In order to reduce the influences of barite and chlorine, we select well A with fresh mud and low formation water salinity. The mud in the borehole has no barite, and the formation containing elements Mg, Al, and K, is more complex than the simulation model used to determination of corrections. The constrained and weighted least-squares method is used to analyze capture gamma-ray energy spectra data of GEM tool to get relative yields of Si, Ca, Fe, and S. The correction of iron yields was done for the residual contribution from stainless steel in the tool. Then, these yields were converted into dry weights, as shown in Fig. 11. The solid lines represent elemental dry weights after correcting for influences of elements Mg, Al, and K based on elemental dry

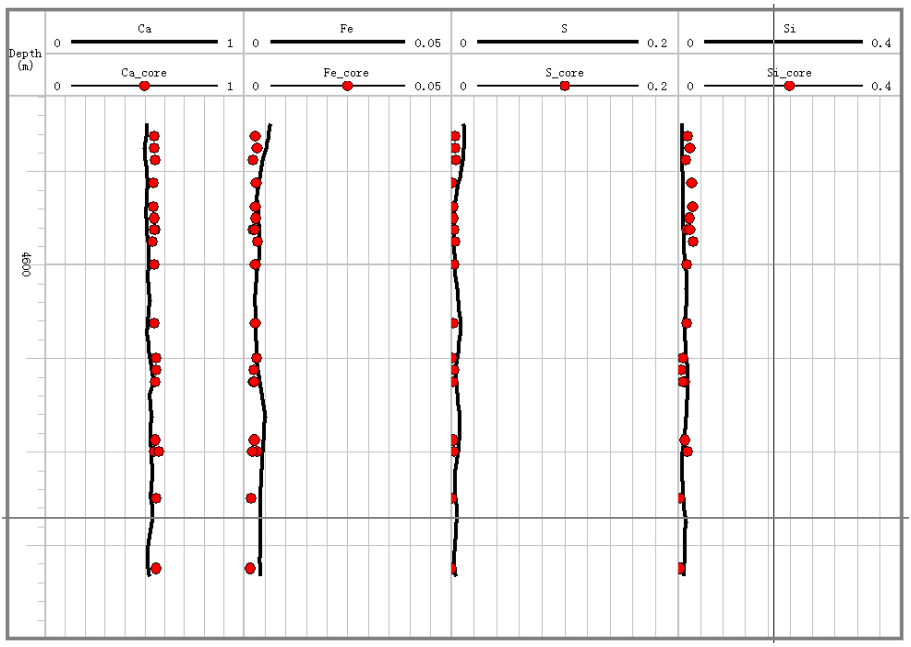

Fig. 11. Influences of Mg, Al, and K, and corrected real well data.

weights derived from spectral analysis using the constrained and weighted least-squares method; the discrete data points are real dry weights of elements derived from core experimental measurement. Before the corrections for the influences of Mg, Al, and K, we find that the calculated dry weight of Si is almost immune to, and the dry weights of Ca and Fe are less affected by Mg, Al, and K, whereas the dry weight of S is the most influenced and deviate from the real values greatly. After the corrections, the real sulfur dry weights derived from core experiments are closer to the corrected elemental dry weights curve, indicating that the above correction methods are effective.

6. CONCLUSIONS

Spectral analysis of both model formation and real formation demonstrates that, in Am-Be-source chemical elemental logging, elements Al, Mg, and K in the formation will influence the calculation of concentrations of other elements. Mg hardly influences the analysis precision of concentrations of Si, Ca, and Fe and influences S concentration to a certain extent. Al influences the calculation of concentrations of Ca, Fe, and S a little but hardly influences Si. K influences other elements not so distinctly but does influence the S concentration calculation significantly. Such influences can be eliminated by correction to obtain more accurate elemental dry weights.

Acknowledgements. This work was supported by the China Natural Science Fund (No. 41374142) and the Science Foundation of China University of Petroleum (Beijing).

References

Chapman, S., J.L. Colson, B. Everett, C. Flaum, M.M. Herron, R.C. Hertzog, G. Pirie, H. Scott, J.S. Schweitzer, J. La Vigne, J. Querein, and R. Wendlandt (1987), The emergence of geochemical well logging, *Tech. Rev*. **35**, 2, 27-35.

Ellis, D.V., and J.M. Singer (2008), *Well Logging for Earth Scientists*, 2nd ed., Springer, Dordrecht.

Galford, J.E., J.A. Quirein, S. Shannon, J.A. Truax, and J. Witkowsky (2009), Field test results of a new neutron-induced gamma-ray spectroscopy geochemical logging tool. **In:** *Proc. SPE Ann. Technical Conference and Exhibition, 4-7 October, 2009, New Orleans, USA*, Society of Petroleum Engineers, DOI: 10.2118/123992-MS.

Grau, J.A., and J.S. Schweitzer (1989), Elemental concentrations from thermal neutron capture gamma-ray spectra in geological formations, *Nucl. Geophys*. **3**, 1, 1-9.

Helmer, R.G., R.L. Heath, L.A. Schmittroth, G.A. Jayne, and L.M. Wagner (1967), Analysis of gamma-ray spectra from NaI(Tl) and Ge(Li) spectrometers. Computer programs, *Nucl. Instrum. Methods* **47**, 2, 305-319, DOI: 10.1016/0029-554X(67)90445-4.

Herron, M.M. (1986), Mineralogy from geochemical well logging, *Clays Clay Miner*. **34**, 2, 204-213, DOI: 10.1346/CCMN.1986.0340211.

Herron, M.M., S.L. Herron, J.A. Grau, N.V. Seleznev, J. Philips, A. El Sherif, S. Farag, J.P. Horkowitz, T.J. Neville, and H. Kai (2002), Real-time petrophysical analysis in siliciclastics from the integration of spectroscopy and triple-combo logging. **In:** *Proc. SPE Ann. Technical Conference and Exhibition, 29 September – 2 October 2002, San Antonio, USA*, Society of Petroleum Engineers, DOI: 10.2118/77631-MS.

Herron, S.L., and M.M. Herron (1996), Quantitative lithology: An application for open and cased hole spectroscopy. **In:** *SPWLA 37th Ann. Logging Symp., 16-19 June 1996, New Orleans, USA*, Society of Petrophysi- cists and Well-Log Analysts, SPWLA-1996-E, 14 pp.

Hertzog, R., L. Colson, O. Seeman, M. O'Brien, H. Scott, D. McKeon, P. Wraight, J. Grau, D. Ellis, J Schweitzer, and M. Herron (1989), Geochemical logging with spectrometry tools, *SPE Formation Eval*. **4**, 2, 153-162, DOI: 10.2118/16792-PA.

Pang, J.F. (1991), *γ-Ray Spectrum Data Analysis*, Shanxi Science & Technology Press, Xi'an (in Chinese).

Pemper, R.R., A. Sommer, P. Guo, D. Jacobi, J. Longo, S. Bliven, E. Rodriguez, F. Mendez, and X. Han (2006), A new pulsed neutron sonde for derivation of formation lithology and mineralogy. **In:** *Proc. SPE Ann. Technical Conference and Exhibition, 24-27 September 2006, San Antonio, USA*, Society of Petroleum Engineers, DOI: 10.2118/102770-MS.

Radtke, R.J., M. Lorente, B. Adolph, M. Berheide, S. Fricke, J. Grau, S. Herron, J. Horkowitz, B. Jorion, D. Madio, D. May, J. Miles, L. Perkins, O. Philip, B. Roscoe, D. Rose, and Ch. Stoller (2012), A new capture and inelastic spectroscopy tool takes geochemical logging to the next level. **In:** *SPWLA 53rd Ann. Logging Symp., 16-20 June 2012, Cartagena, Colombia,* Society of Petrophysicists and Well-Log Analysts, SPWLA-2012-103, 16 pp.

Sweezy J.E., T.E. Booth, and F.B. Brown (2004), MCNP-A general Monte Carlo N-particle transport code. Version 5, MCNP user manual, LA-UR-03-1987, Los Alamos National Laboratory, Los Alamos, USA.

Received 12 November 2013
Received in revised form 28 March 2014
Accepted 25 April 2014